

# Formation of Structured Low-Ohmic p-Type Contacts on Al-Implanted 4H-SiC by Laser Annealing

Carsten Hellinger<sup>1,a\*</sup>, Michael Thum<sup>1,b</sup> and Mathias Rommel<sup>1,c</sup>

<sup>1</sup>Fraunhofer Institute of Integrated Systems and Device Technology (IISB)  
Schottkystrasse 10, 91058 Erlangen, Germany

<sup>a</sup>carsten.hellinger@iisb.fraunhofer.de, <sup>b</sup>michael.thum@iisb.fraunhofer.de,  
<sup>c</sup>mathias.rommel@iisb.fraunhofer.de

**Keywords:** Laser annealing, ohmic contact, structured contact, p-type, 4H-SiC

**Abstract.** In this work, a method is presented to form structured low-ohmic p-type contacts on Al-implanted 4H-SiC by laser annealing. A metal layer sequence for p-type contacts suitable for UV laser treatment was developed. Furthermore, a method to protect thermosensitive layers from damages by laser treatment is presented. By structuring the top metallization layer, it is possible to use the metal stack as a self-aligned mask. That makes it possible to laser the entire surface of the wafer, whereby thermosensitive layers are protected from damages by laser annealing by utilizing the optical properties of the individual metal layers. To evaluate the method, TLM structures were electrically characterized. TLM structures were electrically characterized successfully demonstrating the feasibility of the presented approach.

## Introduction

The ohmic contact between the metal contact layer and the semiconductor is of utmost importance for low  $R_{DS,on}$  power electronic devices [1]. Therefore, the fabrication of low ohmic contacts is one of the essential aspects in the manufacturing and development of highly energy efficient SiC power semiconductor devices, especially for vertical devices. For low p-type ohmic contacts on the frontside usually titanium-aluminum compounds are being used for p-type contacts [1, 2, 3]. A following temperature treatment of the metal layer is necessary for the titanium-aluminum layer to react with the SiC substrate. Thereby the semiconductor  $Ti_3SiC_2$  is formed, which results in a low-ohmic contact on p-type 4H-SiC [1, 4, 5]. This temperature step is generally performed by RTA (rapid thermal annealing) [1], although laser processing of full-surface n-type backside contacts is now established [6, 7, 8]. However, laser annealing for alloying structured frontside contacts is difficult. Either only the ohmic contact areas are annealed, which requires good alignment of metallized areas and laser processing, or the entire surface is annealed, which can lead to damage or degradation of the layers outside the contact area. Another challenge is the laser processing of the titanium-aluminum layer itself. According to literature, a commonly used metal stack for the fabrication of p-type contacts is 300 nm Al / 80 nm Ti, resulting in a  $Ti_3SiC_2$  layer after an annealing step [1]. However, aluminum has a reflectivity of over 90 % at a wavelength of 355 nm [9], which is the wavelength of commonly used short-pulse lasers [8]. As a result, only a small part of the laser radiation is absorbed and the metal layer hardly heats up. Therefore, a different layer composition or layer sequence must be used to produce p-type contacts using laser processing.

In this work, a solution was developed to produce structured ohmic contacts on p-type SiC using laser annealing. For this purpose, Ni / Al / Ti metal stacks were investigated for p-type contact formation by laser annealing. To characterize resulting contacts electrically, TLM structures were prepared, measured and analyzed.

## Experimental

TLM structures were manufactured on a commercial 150 mm 4H-SiC wafer with a n-type epitaxial layer of 10  $\mu\text{m}$  thickness and  $8 \cdot 10^{15} \text{ cm}^{-3}$  doping concentration. The layout of the TLM test structures is shown in fig. 1. Al was implanted in the area of the TLM structures (see fig. 1 with a surface

concentration of approx.  $5E19 \text{ cm}^{-3}$  using three individual ion implantation steps (see table 1). To activate the dopants the wafers were subsequently annealed at  $1700^\circ\text{C}$  for 30 minutes in Ar atmosphere.

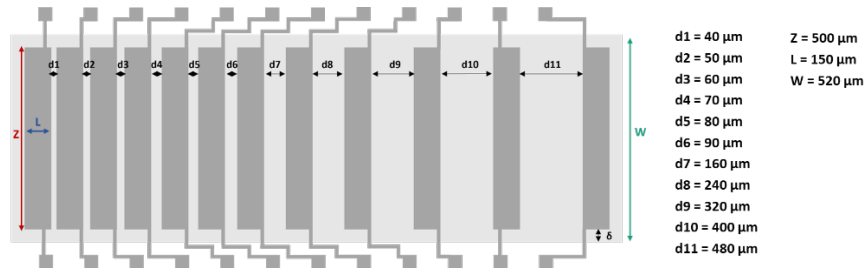


**Fig. 1.** TLM test structures in top view, where Z is the width and L the length of the TLM pattern, W the wide of the implanted tub and d the distance between the TLM pattern (dark grey: contact structures, light grey:  $p^+$ -doped area).

**Table 1.** Parameters of p-type implantation.

Energy [keV]	Dose [ $1/\text{cm}^2$ ]
90	$2.8E14$
60	$1.8E14$
30	$1.4E14$

Afterwards the metallization layer was deposited. Therefore, a stack of 20 nm Titanium and 75 nm Aluminum was evaporated and a photoresist was spin coated and structured, before the uppermost 20 nm Ni layer was deposited (see fig. 2). Then the uppermost Ni layer was structured by lift-off (see fig. 3a) and the whole wafer was laser annealed with different energy densities. Therefore a Sumitomo SWA20US-M laser annealing tool with a frequency-tripled Nd:YVO<sub>4</sub> laser with 355 nm wavelength, a beam size of  $80 \mu\text{m}$  and a pulse duration of 50 ns was used. The energy density was varied from 1.4 to  $2.8 \text{ J}/\text{cm}^2$ , whereby the overlap in x-direction was varied from 67 to 80 % and in y-direction from 50 to 80 %.

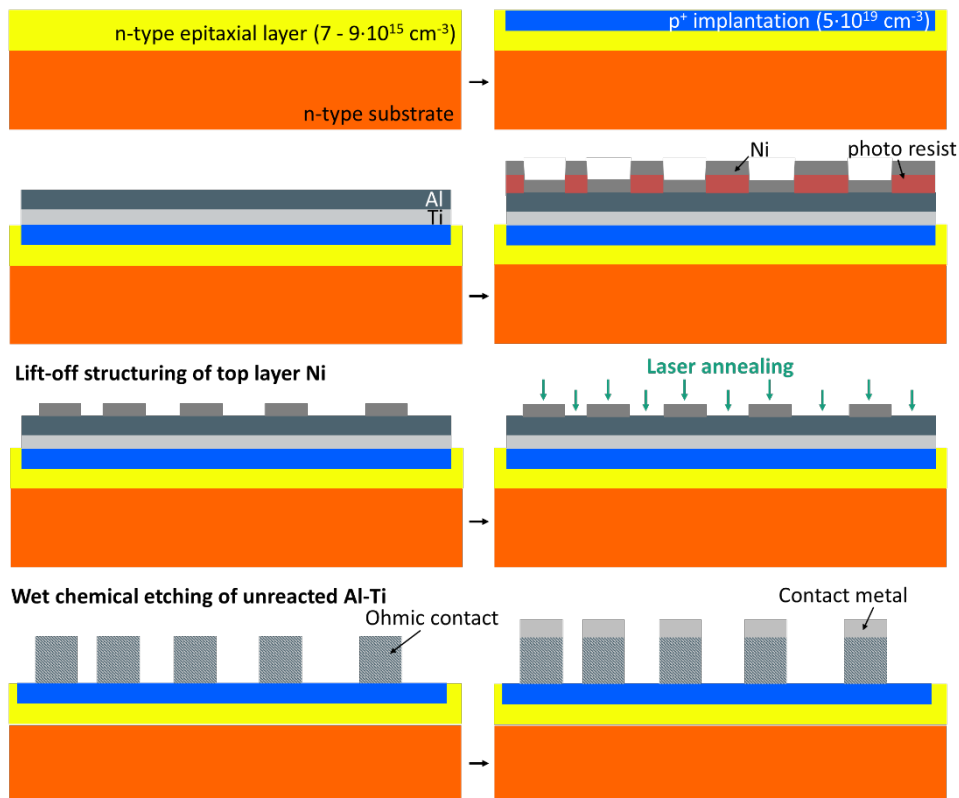


**Fig. 2.** Process flow to produce TLM structures.

Since the used Ni (20 nm) / Al (75 nm) / Ti (20 nm) stack has only a reflectivity of 43 % [10] compared to Aluminum with over 90 % at 355 nm [9], significantly more radiation is absorbed in the ohmic contact areas with Ni layer on top, causing a reaction of the metal layers with the SiC substrate (see fig. 3b). In the area between the contacts, however, where aluminum is the top layer, most of the radiation is reflected and no reaction takes place until very high energy densities are being used for the laser annealing (see fig. 3b). After irradiation the non-reacted Al-Ti-layer between the ohmic contact areas was removed wet-chemically (see fig. 3c and fig. 4). Finally, a titanium and platinum layer is deposited and structured as contact metal.

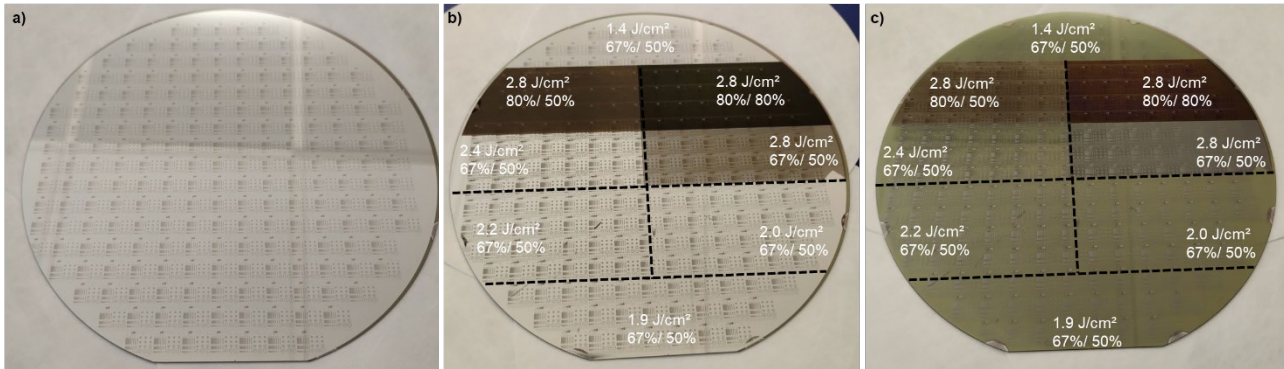


**Fig. 3.** Images of TLM structures after (a) lift-off, (b) laser annealing with different energy densities and overlaps and (c) wet chemical etching of unreacted Aluminum and Titanium.

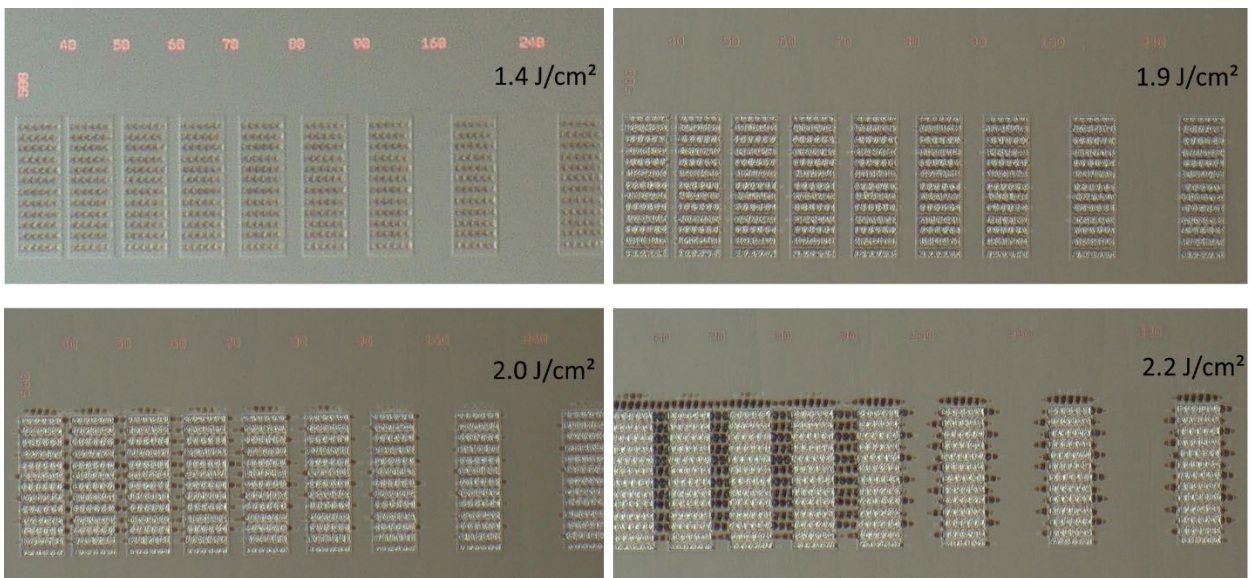


**Fig. 4.** Microscope images of lasered TLM structures depending on energy densities after wet chemical etching of unreacted aluminum and titanium.

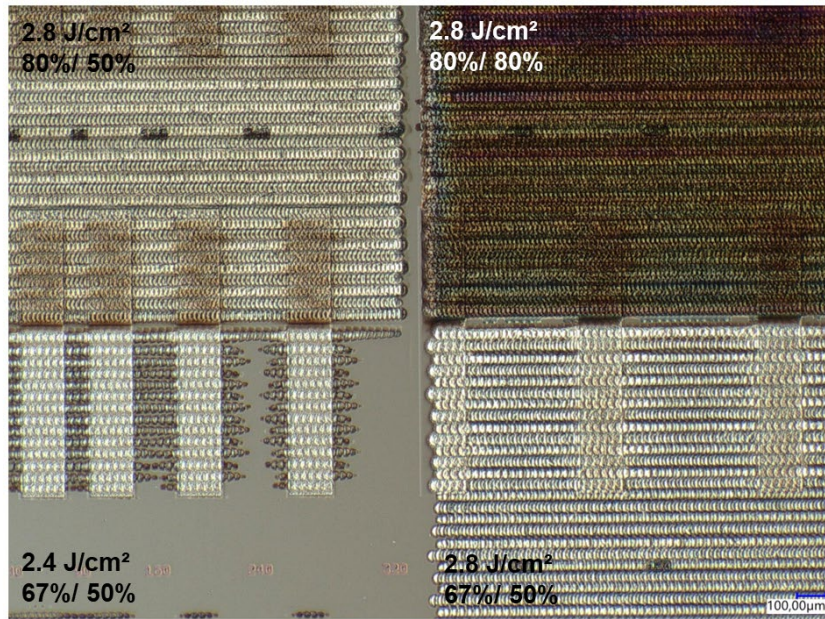


**Fig. 5.** Microscope images of lasered TLM structures depending on energy densities and laser spot overlap in x- and y-direction after wet chemical etching of unreacted aluminum and titanium.

## Results and Discussion

The optical analysis of the samples (fig. 4 and 5) shows that the reflectivity of the aluminum layer is high enough at 355 nm wavelength for energy densities up to 2.4 J/cm<sup>2</sup>. The non-reacted metal can be completely removed after thermal treatment. For higher energy densities, the metallization between the TLM structures reacts with the silicon carbide substrate and could not be etched wet-chemically. This means that the TLM patterns are short-circuited. For energy densities of 2.2 and 2.4 J/cm<sup>2</sup> it is noticeable that the lateral spread of the contacts is increased beyond the original contact length  $L$  after laser treatment (see fig. 4 and 5). For 2.2 J/cm<sup>2</sup>, the contacts up to 90  $\mu\text{m}$  apart and for 2.4 J/cm<sup>2</sup> the contacts up to 160  $\mu\text{m}$  apart are short-circuited. Also, for 2.0 J/cm<sup>2</sup> a lateral spread can be seen in fig. 4. This observation and the associated reduction in the distance between the TLM patterns must be considered when evaluating the  $I(V)$  characteristics. Fig. 6 exemplary shows the resistance as a function of the distance between the TLM patterns for different energy densities and a linear fit. Only the non-short-circuited TLM patterns were used for the evaluation and the distance between the TLM patterns was corrected according to the lateral spread. The fit line shows a high coefficient of determination. It can be used to calculate the sheet resistance and the specific contact resistance.

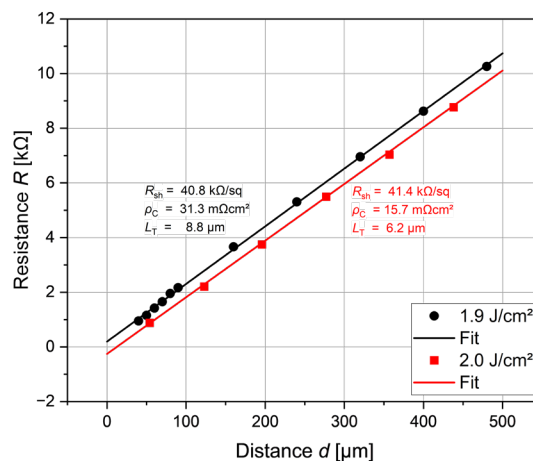


**Fig. 6.**  $R(d)$  plot for an exemplary TLM test structure as a function of energy density.

Fig. 7 shows the specific contact resistivity and sheet resistance for different energy densities. The sheet resistance depends on the dopant concentration [11]. Since all test structures were produced according to the implantation values in table 1, the sheet resistance should be independent of the energy densities during the laser treatment. Due to the significantly large lateral spread, only the values for energy densities lower than  $2.4 \text{ J/cm}^2$  are plotted. The specific contact resistivity shows the lowest values with  $29.5 \pm 11.3 \text{ m}\Omega\text{cm}^2$  for  $1.9$  and  $31.9 \pm 5.0 \text{ m}\Omega\text{cm}^2$  for  $2.0 \text{ J/cm}^2$  in average. At  $1.4 \text{ J/cm}^2$ , the energy density does not appear to be high enough to produce low-resistance contacts as the average specific contact resistivity is  $234.0 \pm 8.0 \text{ m}\Omega\text{cm}^2$ . For  $2.2 \text{ J/cm}^2$ , the average specific contact resistivity is  $253.5 \pm 64.4 \text{ m}\Omega\text{cm}^2$  and is more than eight times higher than for  $1.9 \text{ J/cm}^2$ . At the same time, the test structures with  $2.2 \text{ J/cm}^2$  have significantly higher standard errors. Due to the manual insertion of the wafer into the laser tool, it is possible that the transitions between the sectors with  $2.2 \text{ J/cm}^2$  and  $2.4 \text{ J/cm}^2$  do not correspond exactly to the mask layout, whereby structures in the transition were processed with the surrounding energy densities (see fig. 5) and consequently falsify the measurement results.

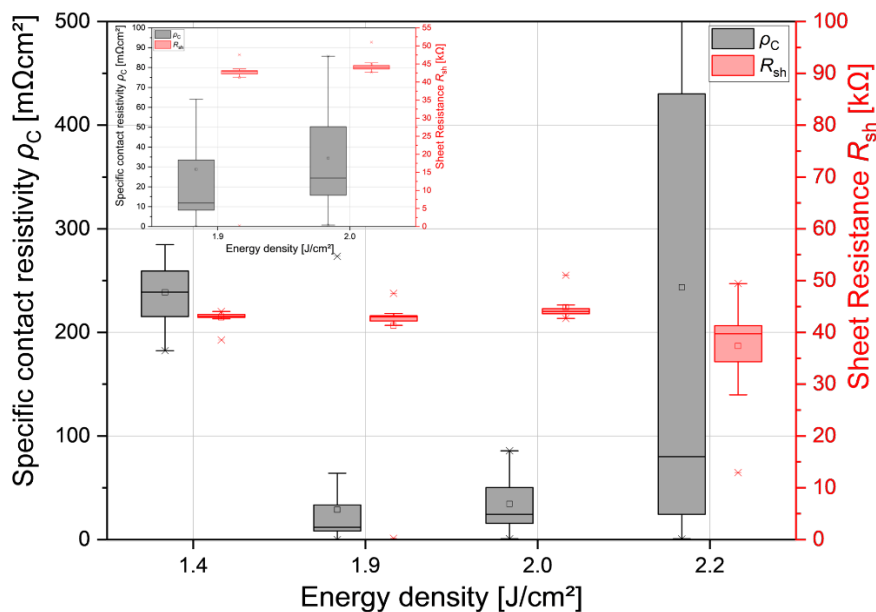


**Fig. 7.** Determined specific contact resistivity and sheet resistance depending on energy density.

To further narrow down the process window for the laser parameters and metal stack thicknesses to optimize the specific contact resistance, further tests are necessary. To find out which reaction products, i.e.  $\text{Ti}_x\text{SiC}_y$  and  $\text{Ni}_x\text{Si}_y$  compounds, are responsible for the ohmic contact formation additional XRD and TEM analyses are essential.

## Summary

In this work, titanium-based ohmic contacts were produced on p-doped 4H-SiC using a UV short pulse laser. Due to the optical properties of the commonly used Al (300 nm) / Ti (80 nm) metal stack a novel Ni (20 nm) / Al (75 nm) / Ti (20 nm) stack optimized for UV lasers was used, whereby the Ni layer was structured by lift-off. The use of the structured metal stack as a self-aligned mask makes it possible to laser the entire surface of the wafer, whereby thermosensitive layers are protected from damages by laser annealing by utilizing the high reflectivity of the top Al layer, where the Ni was removed. With this method contact pads with a size between  $0,01 \text{ mm}^2$  and  $0.3 \text{ mm}^2$  could be realized. It was shown that structured contacts with a specific contact resistance of  $29.5 \text{ m}\Omega\text{cm}^2$  for  $1.9 \text{ J/cm}^2$  and  $31.9 \text{ m}\Omega\text{cm}^2$  for  $2.0 \text{ J/cm}^2$  on average on p-doped 4H-SiC could be produced using this method.

**References**

- [1] T. Kimoto and J. Cooper. *Fundamentals of Silicon Carbide Technology: Growth, Characterization, Devices and Applications*, IEEE Press, Wiley, Singapore (2014).
- [2] F. Roccaforte et al. Critical issues for interfaces to p-type SiC and GaN in power devices. *Appl. Surface Science* 258, 2012
- [3] T. Abi-Tannous et al. A Study on the Temperature of Ohmic Contact to p-type SiC based on  $Ti_3SiC_2$  Phase. *IEEE Transactions on Electron Devices* 63, 2016
- [4] M. Gao et al. Role of Interface Layers and Localized States in TiAl-based Ohmic Contacts to p-type 4H-SiC. *Journal of Electronic Materials* 36, 2007
- [5] C.A. Fisher and M.R. Jennings. On the Schottky Barrier Height Lowering Effect of  $Ti_3SiC_2$  in Ohmic Contacts to p-type 4H-SiC. *International Journal of Fundamental Physical Sciences*, 2014
- [6] R. Rupp, R. Kern and R. Gerlach. *Laser backside contact annealing of SiC Power devices: A Prerequisite for SiC thin wafer technology*. Kanazawa, Japan: Wiley IEEE, IEEE Xplore, 2014
- [7] O. Rusch et al. Reducing On-Resistance for SiC Diodes by Thin Wafer and Laser Anneal Technology, *Material Science Forum* 1004 (2020).
- [8] G. Li et al. Fabrication of Ohmic Contact on N-Type SiC by Laser Annealed Process: A Review, *Crystals* 13(7):1106 (2023)
- [9] A. D. Rakić. Algorithm for the determination of intrinsic optical constants of metal films: application to aluminum, *Appl. Opt.* 34, 4755-4767 (1995).
- [10] A. D. Rakić, A. B. Djurišić, J. M. Elazar and M. L. Majewski. Optical properties of metallic films for vertical-cavity optoelectronic devices, *Appl. Opt.* 37, 5271-5283 (1998).
- [11] D. K. Schroder. *Semiconductor material and device characterization*. Wiley-Interscience IEEE Press, Hoboken, N.J, Piscataway, NJ, (2006)